The influence of solution viscosities and surface tension on calcium-alginate microbead formation using dripping technique

Fatma Davarcı [a], Deniz Turan [a], Beraat Ozcelik [a, *], Denis Poncelet [b, **]

[a] Istanbul Technical University, Faculty of Chemical and Metallurgical Engineering, Department of Food Engineering, Ayazağa Campus, 34469 Maslak, Istanbul, Turkey
[b] Oniris, UMR CNRS 6144 GEPEA, Rue de la Géraudière, CS 82225, 44332 Nantes Cedex 3, France

A B S T R A C T

Currently, there is a growing interest for encapsulation of bioactive ingredients using calcium alginate microspheres or beads. Diffusion of the Ca in the alginate droplets provokes an ionic gelation and their conversion to hydrogel beads. The main objective of this study is to investigate the influence of physical properties of alginate and $CaCl_2$ solutions on alginate droplet formation and penetration into gelling bath, in size and shape of Ca-alginate beads. The droplet formation and penetration in the calcium bath was investigated using a high-speed video recording. Viscosity of alginate solution was modified by changing the alginate concentration (from 10 to 30 g/L) and the viscosity of the bath was modified by using different water/glycerol mixes (0—90% of glycerol) to prepare the $CaCl_2$ solution. Surface tension of $CaCl_2$ solution is reduced by adding different concentrations of surfactants (Tween 20) in a range of 0.01 −1 g/L. Droplets detach from the tip with a tear shape. In all conditions tested, the droplets reach a spherical shape in less than 15 ms after detachment and less than 25 mm from the tip. Spherical beads are obtained when the kinetic energy is high enough to break the surface resistance of the calcium bath and droplet viscosity high enough to avoid deformations. Penetration depth of alginate droplets were mainly affected by viscosity and surface tension of $CaCl_2$ solution. When viscosity and surface tension of $CaCl_2$ solution increases, sphericity decrease and shape deformations are observed. The surfactant addition enhanced penetration and prevented shape deformations of Ca-alginate beads.

© 2016 Published by Elsevier Ltd.

1. Introduction

Bioencapsulation is defined as the process of confining bioactive compounds (e.g. microbial cells, enzymes, animal cells, plant cells, antibiotics, etc.) within a matrix in particulate form (i.e. bead or capsule) in order to achieve one or more desirable effects: immobilization, protection, stabilization, controlled-release and/or affect the physical properties of the bioactive compounds (Chan, Lee, Ravindra, & Poncelet, 2009; Doherty et al., 2011). Nowadays, functional foods are new trend for consumers towards a healthier life. Encapsulation technologies are promising alternatives to overcome problems in food industry such as degradation or oxidation of bioactive compound incorporated into food (Akhtar,

Murray, Afeisume, & Khew, 2014; Li et al. 2015; Schrooyen, van der Meer, & De Kruif, 2001; Ubbink & Krüger, 2006). The application of encapsulation in food industry includes the entrapment of bioactive compounds such as antioxidants, vitamins and minerals, essential oils, polyunsaturated fatty acids (PUFAs) mainly n-3 polyunsaturated fatty acids, flavors, enzymes, probiotics, etc., into small capsules (Gibbs et al., 1999; Koupantsis, Pavlidou, & Paraskevopoulou, 2014; Rajabi, Ghorbani, Jafari, Mahoonak, & Rajabzadeh, 2015; Yang & McClements, 2013).

The alginate, a natural polysaccharide, is extensively used as wall material in encapsulation processes due to their non-toxicity, biocompatibility and mild gelling properties (Knezevic et al., 2002). Moreover, sodium alginate is preferentially used as a gelling agent in the food industry mainly due to its high water-solubility (Nakauma et al., 2016). The alginate gel beads are generally produced by extrusion drop-by-drop (dripping) of an alginate solution in gelling calcium bath (Kierstan & Bucke, 2000; Lević, Lijaković, Đorđević, Rac, Rakić, Knudsen, et al., 2015; Zeeb, Saberi, Weiss, & McClements, 2015). Physical characteristics such

as shape and size are important in the consideration of alginate beads properties (Belščak-Cvitanović, Bušić, Barišić, Vrsaljko, Karlović, Špoljarić, et al., 2016; Chan, Lim, Ravindra, Mansa, & Islam, 2012; Nussinovitch, 2010). However, there is limited information on shape deformations of alginate beads, which occurred, in different steps of encapsulation process. Recently, a master shape diagram has been developed to reveal the relationship between the alginate solution variables and the shape of the Ca-alginate large beads formed by the simple extrusion dripping method (Chan et al., 2009).

The main objective of this study is to investigate the alginate droplet formation at nozzle tip, its evolution during falling and penetration in the gelling calcium bath, in function of physical properties such as viscosity and surface tension of alginate and receiving $CaCl_2$ solution using a high-speed camera. Images were captured and analyzed to define bead diameter, sphericity and shape deformations during the different steps of the bead production.

2. Materials and methods

2.1. Materials

Sodium alginate powder ALGOGEL 3001 (molecular weight: 151,200 Da) was obtained from Cargill (France). Algogel 3001 has a high guluronic acid content (M/G ratio) as 0.64. Calcium chloride dihydrate powder ($CaCl_2.2H_2O$) was purchased from Panreac (Spain). Glycerol used in the study was 99, 5% pure and obtained from Labogros (France). Surfactant (Tween 20) and all the other chemicals used in the study were obtained from Sigma-Aldrich (St. Louis, MO USA).

2.2. Methods

2.2.1. Preparation of alginate solutions
A defined quantity of alginate was spread in a beaker containing 1 L of distilled water under high speed mixing. Then, the mixing speed was reduced and stirring was maintained for 1 h at low speed. Finally, the solutions were left standing for 24 h to remove bubbles before use. To evaluate the impact of the alginate solution viscosity, solutions of 5—35 g/L were prepared.

2.2.2. Preparation of gelling $CaCl_2$ solutions
Twenty g calcium chloride ($CaCl_2.2H_2O$) was introduced in a beaker containing 1 L of an aqueous solution. In order to evaluate the impact of the viscosity of gelling calcium solution, the aqueous solution was prepared by mixing glycerol and water. The concentration of glycerol was varied from 0 to 90% (v/v). In order to observe the influence of surface tension on penetration process, up to 1 g/L Tween 20 was added into $CaCl_2$ solution. In solution series, the calcium concentration was kept constant.

2.2.3. Viscosity measurement of solutions
The viscosities of alginate and $CaCl_2$ solutions were determined by using viscometer (Haake VT 550, USA) using Rheowin Job Manager Software. Fifty ml of solution inserted in the cell. The sample placed into the chamber was subjected to an increase of shear rate from 0 to 300 s^{-1} followed by a decreasing shear rate from 300 to 0 s^{-1}, over 60 s. The reading is done at 200 s^{-1}. During the viscosity measurements, the temperature was kept at 25 °C. All measurements were done as three replicates.

2.2.4. Surface tension measurement of solutions
The surface tensions of solutions were determined by using tensiometer (KRÜSS K-12, France) using du Nouy ring method and LabDeskTM software. For the surface tension measurement, 70 ml of each solution was used for the analysis and the temperature was kept at 25 °C (Lee, Ravindra, & Chan, 2008). All measurements were done as three replicates.

2.2.5. Experimental set-up and production of the alginate beads
Fig. 1 shows the experimental set-up for producing the beads. Alginate solution was filled into a hypodermic syringe (Terumo, Tokyo) which was connected to a syringe pump (KD Scientific, USA). Solution was extruded drop-wise through conical tip of 0.6/0.9 mm internal/external diameter (Norton EFD, Dosage 2000; France) into the $CaCl_2$ bath. A gentle mixing was applied to $CaCl_2$ solution to prevent sticking of the beads.

First, alginate flow rate were changed from 50 to 300 ml/h in order to study the influence of it on bead diameter and sphericity. Then, alginate flow rate was set to 100 ml/h in order to see the influence of viscosity and surface tension of solution. The distance between the nozzle tip and collecting bath was 20 cm. After droplet penetration, beads were let to harden for 30 min to ensure complete gelation. Afterwards, the beads were filtered using a sieve and rinsed with distilled water. Then, beads were hold in $CaCl_2$ solution until size and shape analysis. In order to understand if the falling drop has enough energy to break the surface, kinetic energy was measured and the liquid properties of the gelling bath were not varied this time. The collecting distance between the dripping tip
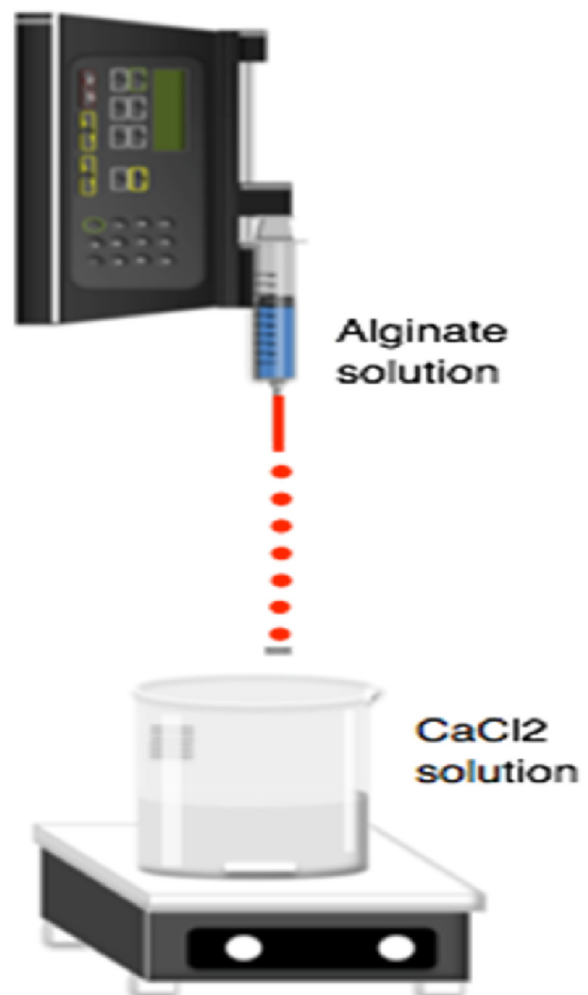

Fig. 1. Schema of the alginate bead production set-up.

and gelation bath was varied from 0 to 270 cm.

2.2.6. Observation of dripping process

Dripping process was divided into three steps.

- droplet formation,
- fall of droplets in air and
- penetration into the bath.

Images were recorded and observed by using a Phantom V 7.3 high-speed camera (Vision Research, USA) at 400 images per second. For all determinations, at least 25 droplets were observed. From the image analysis, falling velocity (V) was evaluated by recording images, measuring the displacement of the droplet over a defined period of time, in function of distance from the tip. The kinetics energy (E) of the droplet was estimated using:

$$E = \frac{1}{2}mV^2 \qquad (1)$$

where the mass of the droplet is equal to:

$$m = \frac{\pi}{6}d^3\rho \qquad (2)$$

where d is the mean diameter of the droplet and ρ is the solution density.

Similarly, penetration depth was determined by recording images with the high-speed video camera and recording the maximum depth reached by the droplet in the bath.

2.2.7. Bead characterization

Morphological observations and size analysis of the beads were realized using a digital microscope (Dino-Lite, Netherlands). The maximum and minimum diameters (d_{max}, d_{min}) were measured. The average size and standard deviation of the beads were computed from at least 25 beads from each batch randomly selected.

The sphericity factor (Φ) of alginate beads is estimated using the following formula:

$$\Phi = \frac{2d_{min}}{d_{min} + d_{max}} \qquad (3)$$

For $\Phi > 0.95$, beads were considered spherical or slightly oval. For $0,95 > \Phi > 0.90$, beads were considered oval and pear shape. Lower values mean significant, i.e. unacceptable, shape deformations.
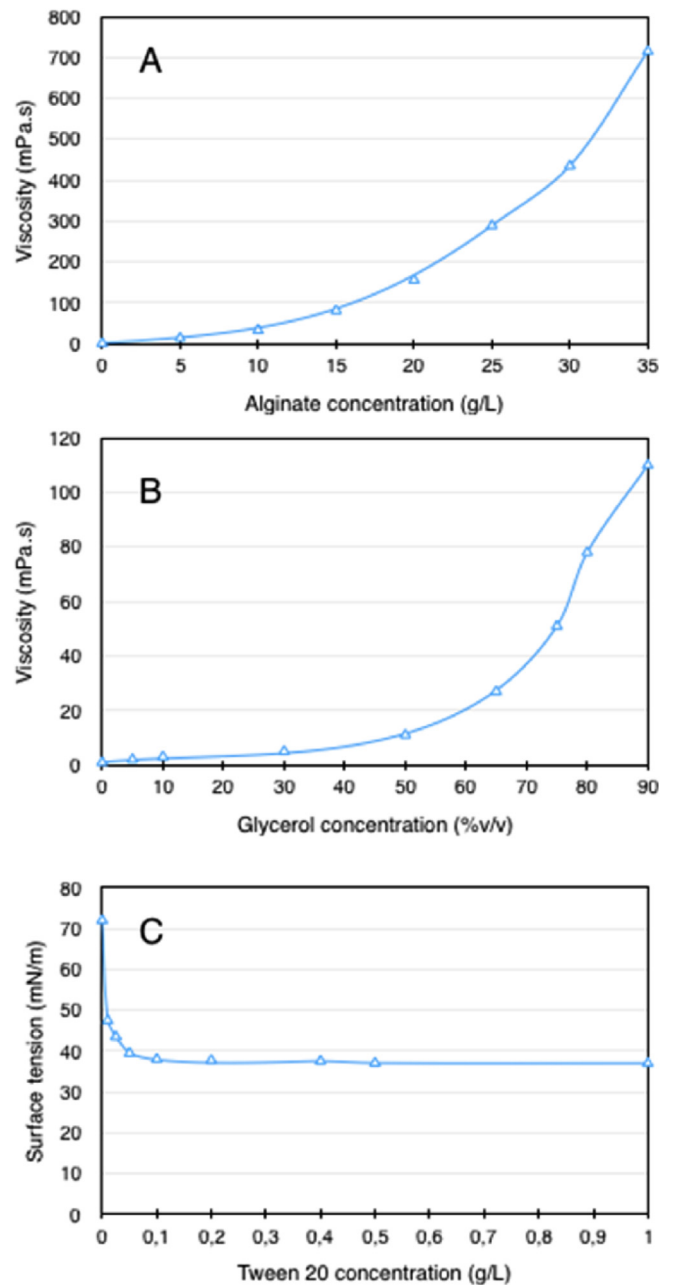
2.2.8. Statistical analysis

All the given values are the average of results obtained from three replicates of analysis. Standard deviations are also given with the values. For the statistical analysis SPSS v.15 statistics program (SPSS Inc., Chicago, USA) was used. Data that prepared using Microsoft® Office Excel 2007 were transferred to SPSS and analysis of variance (ANOVA) was performed. Statistically difference ($p < 0.05$) was evaluated by Duncan's multiple-range test.

3. Results and discussion

3.1. Viscosity measurement of solutions

The results of viscosity measurement of alginate solutions prepared at various concentrations are given in Fig. 2a. The alginate viscosity from 5 g/L to 35 g/L alginate concentration was obtained, 13 ± 1 to 715 ± 4 mPa s, in an exponential manner. This is in good

Fig. 2. Viscosity graph of alginate solutions prepared at different concentrations (a); viscosity graph of CaCl$_2$ bath prepared with different water/glycerol solution (b); surface tension graph of CaCl$_2$ solutions prepared by adding different concentrations of Tween 20 (c).

agreement with the previous studies (Chan et al., 2009). Previous studies have shown that the alginate solution viscosity must be above 60 mPa s to produce beads with good mechanical properties and desired spherical shape. Alginate solutions having too high viscosities (>500 mPa s) are difficult to pump and cause shape deformations on beads (Moghadam, Samimi, Samimi, & Khorram, 2008). In the present paper, the alginate concentration was then limited 10–30 g/L, corresponding to the viscosity range was measured as 33–453 mPa s.

Glycerol was commonly used to alter the viscosity of aqueous solutions. As glycerol concentration in CaCl$_2$ solution increased, the viscosity of the solution increased in an exponential manner (Fig. 2b) from 1 to 110 mPa s, corresponding to 0–90% (v/v) glycerol

Table 1
Diameter of Ca-alginate beads (mm) produced by using different alginate concentrations and $CaCl_2$ gelling bath composition.

Surface tension of $CaCl_2$ solution (mN/m)	Alginate viscosity and concentration				Mean
	33 mPa s 10 g/L	81 mPa s 15 g/L	156 mPa s 20 g/L	435 mPa s 30 g/L	
72.27	2.96 ± 0.09	3.07 ± 0.05	3.11 ± 0.04	3.12 ± 0.03	3.06[a]
47.55	2.96 ± 0.05	3.05 ± 0.05	3.10 ± 0.03	3.12 ± 0.04	3.06[a]
43.32	2.95 ± 0.06	3.05 ± 0.05	3.10 ± 0.03	3.11 ± 0.05	3.05[a]
39.48	2.96 ± 0.05	3.05 ± 0.04	3.11 ± 0.04	3.14 ± 0.03	3.06[a]
38.08	2.95 ± 0.04	3.06 ± 0.04	3.09 ± 0.04	3.14 ± 0.03	3.06[a]
37.05	2.93 ± 0.05	3.06 ± 0.05	3.10 ± 0.03	3.11 ± 0.05	3.05[a]
Mean	2.95[A]	3.06[B]	3.10[C]	3.12[D]	
Viscosity of the $CaCl_2$ solution (mPa.s)					
1	2.95 ± 0.12	3.03 ± 0,.05	3.04 ± 0.05	3.12 ± 0.05	3.03[a]
2	2.93 ± 0.11	3.03 ± 0.07	3.03 ± 0.06	3.12 ± 0.05	3.03[a]
3	2,92 ± 0.10	3.01 ± 0.07	3.03 ± 0.04	3.09 ± 0.06	3.01[a]
5	2.90 ± 0.12	2.92 ± 0.08	2.99 ± 0.09	3.09 ± 0.03	2.97[b]
11	2.84 ± 0.21	2.77 ± 0.08	2.87 ± 0.08	2.97 ± 0.08	2.87[c]
27	2.72 ± 0.23	2.70 ± 0.12	2.74 ± 0.19	2.87 ± 0.08	2.78[d]
82	–	2.50 ± 0.19	2.50 ± 0.12	2.57 ± 0.15	2.52 [e]
110	–	–	2.49 ± 0.14	2.52 ± 0.14	2.51[e]
	2.89[A]	2.85[B]	2.84[B]	2.92[A]	

* Different lowercase letters in mean column (group comparisons were performed only regarding the surface tension of $CaCl_2$) and uppercase letters in mean row (group comparisons were performed only regarding the concentration of alginate) indicate statistically significant differences at 5% ($p < 0.05$) according to Duncan's test.
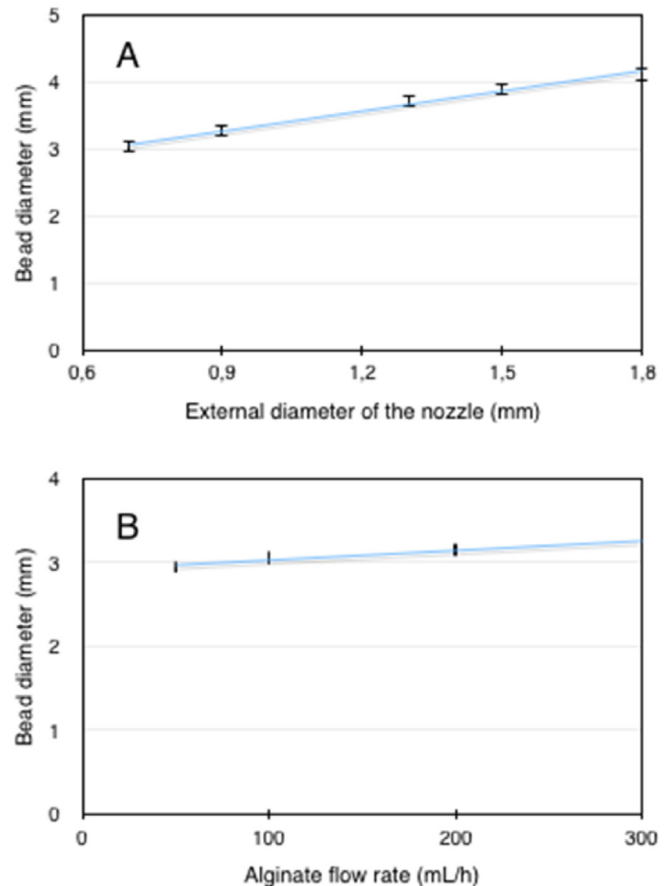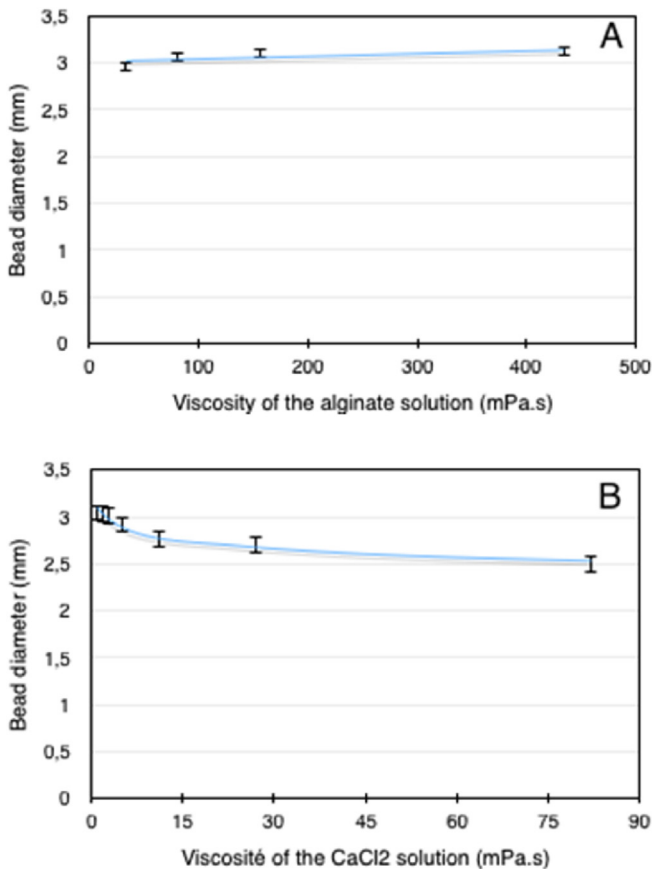
into 20 g/L $CaCl_2$ solution.

3.2. Surface tension of solutions

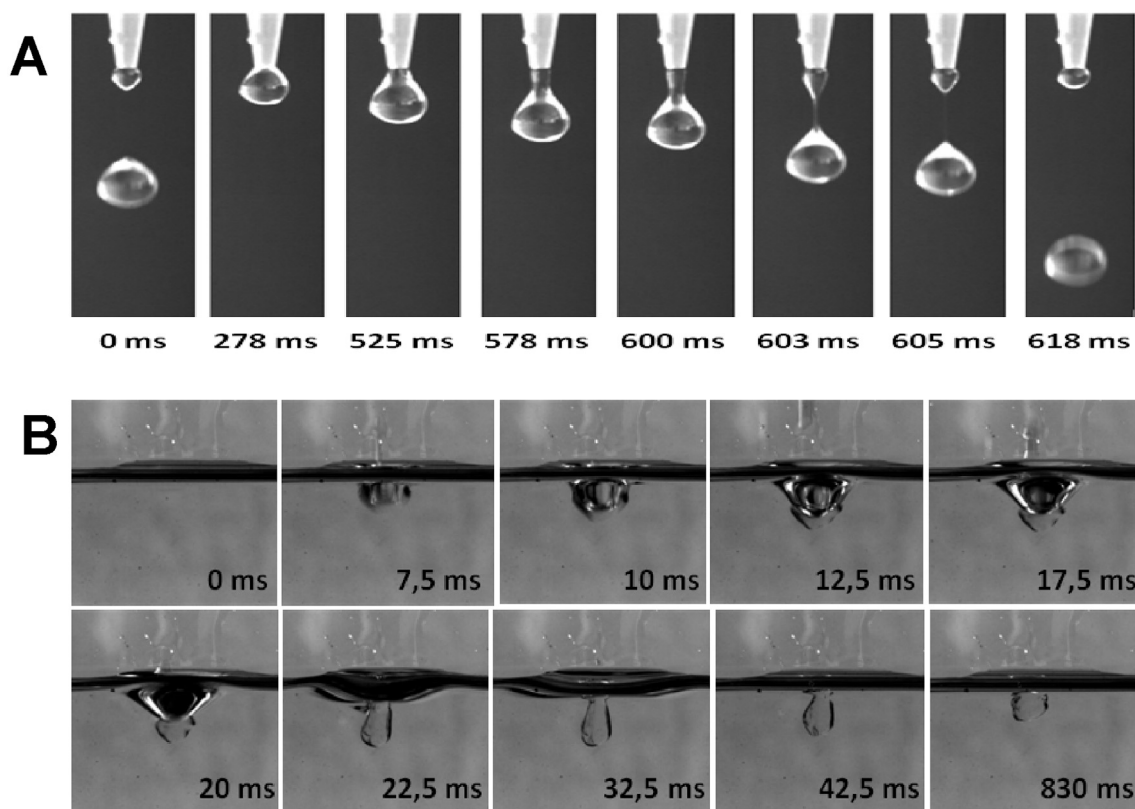The surface tension is not significantly modified by the addition of alginate to water (Chan et al., 2009). Moreover, a static measurement of the surface tension is probably not fully representative of the behavior during droplet formation and penetration. Thus, the influence of surface tension of alginate solution is neglected in the study.

Surface tension of water was measured and found as 72 mN/m

Fig. 3. Effect of viscosity of alginate (a) and $CaCl_2$ gelling solution (b) on bead diameter (Error bars indicate the standard deviation).

Fig. 4. Influence of the external nozzle diameter (a) and alginate flow rate (b) on the bead diameter (Error bars indicate the standard deviation).

Fig. 5. Image sequence of alginate (20 g/L) droplet formation. Time in millisecond from the beginning of formation to the detachment of the droplet (a); poor penetration and shape deformation of alginate (20 g/L) droplet at high CaCl₂ viscosity (110 mPa.s) during penetration step (b).

as reported in the literature. Dissolved salts usually increase the surface tension of water (Boström, Kunz, & Ninham, 2005). The surface tension at 20 g/L CaCl₂ solution was not found significantly higher than surface tension of water. As the Tween 20 concentration in CaCl₂ solution increased, surface tension of solution decreases until reaching the critical micelle concentration (CMC) (Fig. 2c). CMC of Tween 20 was found around 0.05 g/L, in accordance to literature data 0.044–0.058 g/L (Pennell et al., 2000). The surface tension of CaCl₂ solution is reduced from 72 mN/m to around 37 mN/m by adding 0.01–1 g/L Tween 20.

3.3. Diameter of alginate beads

The size of the alginate beads was determined over more than 60 experiments made in triplicate by modifying the concentrations of alginate, the size of the nozzle and the flow rate of the alginate solution, Tween 20 and glycerol concentration in the bath (Table 1). Contraction was assumed independent of the alginate solution and CaCl₂ formulation. Size of beads is then proportional to the initial droplet.

Viscosity of the alginate solution (and its concentration) has a statistically significant but limited influence on the bead diameter (Table 1, Fig. 3a). The diameter of the beads is not impacted by the presence of Tween 20 in the bath (Table 1). Bead diameter decreases as the glycerol concentration increases (Table 1 and Fig. 3b). This result might be due to the osmotic effect of glycerol. Adding glycerol to the CaCl₂ gelling bath created an osmotic pressure, thus beads lost water towards to the medium leading to additional shrinkage to the contraction and resulted in smaller bead diameter. However, this osmotic effect must not affect the droplet formation it-self, its falling and its penetration in the CaCl₂ gelling bath.

Fig. 4a shows that the bead diameter increases with the nozzle external diameter. This is an agreement with Tate's law (Harkins & Brown, 1919):

$$\frac{\pi}{6}d^3 \rho \, g = \pi d_e \gamma \tag{4}$$

Where d is the droplet diameter, ρ the solution density, g the gravity constant, d_e the external diameter of the nozzle and γ the alginate surface tension. The size of the droplet increases with the alginate flow rate (Fig. 4b). This effect is mainly linked to the fraction of the neck remain attached on the nozzle when the droplet detaches (see droplet formation below).

3.4. Droplet formation

Droplet formation at nozzle tip is the first step of dripping technic. This droplet formation was observed by using a high-speed camera and could be divided as follows (Fig. 5a):

- Polymer liquid flows through the nozzle tip forming small relatively spherical shape (278 ms)
- Due to gravity forces, as the droplet grows it takes a pear or tear shape (525 ms)
- The deformation leads a neck which still maintains the droplet on tip (578 and 600 ms)
- The neck elongates until it breaks (603 ms)
- The droplet detaches with pear shape, while a small part of the neck remains on the tip (605 ms)
- In less than 15 ms, the falling droplet moves to a spherical form (618 ms).
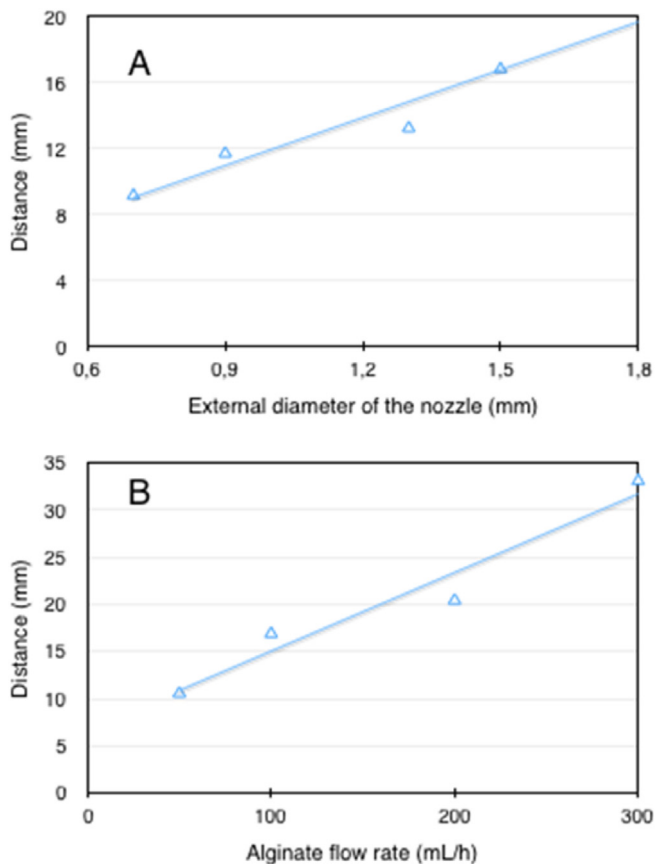
Fig. 6. Minimum falling distance to obtain spherical droplets versus nozzle diameters (a) and flow rates (b); Alginate solution 20 g/L.
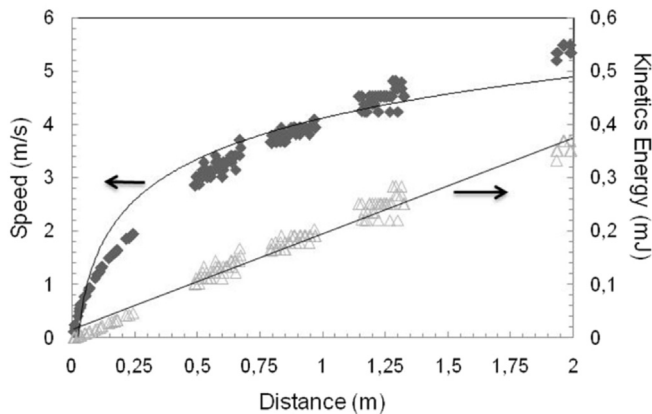

Fig. 7. Kinetic energy and velocity of falling alginate (20 g/L) droplet.

An interval between droplets, i.e. formation of the neck and detachment of the droplet varies between 400 and 1200 ms and depends on the nozzle size and the alginate flow rate. Alginate droplets detached from the nozzle tip with tear-shaped. Due to the surface tension forces, in less than 20 ms, droplets evolve to spherical shape.

Analyzing the video recorded images (Fig. 5a); it was possible to define the minimum distance from the nozzle to get spherical droplets. This distance was not impacted by the alginate concentration or viscosity of the alginate. However, the droplets become spherical at a longer distance of the nozzle when the nozzle

diameter and alginate flow rate increase (Fig. 6a and b). In both cases, the length of the droplet neck before detachment from the tip is effective rather than the time passed for spherical droplet shape forming from pear shape.

Even with a large tip diameter and high flow rate, the distance to get spherical droplets was less than 2.5 cm and the time less than 1–2 s. Droplets are generally formed with the tip diameter less than 1 mm, leading to a usual time and distance lower than 500 ms and 1 cm respectively. It may then be concluded that, in practical conditions, droplets are spherical before to reach the $CaCl_2$ gelling bath surface.

3.5. Droplet falling velocity and kinetics energy

To penetrate in the $CaCl_2$ gelling bath, droplets must have enough energy to break the surface of the bath. To evaluate the kinetic energy of the droplet, droplet velocity (V, m/s) was calculated by measuring the distance covered by the droplets during a certain time. The kinetics energy (E, J) was then computed based equations (1) and (2).

Fig. 7 shows a typical evolution of the falling velocity and kinetics energy in function of the distance from the tip. The theoretical terminal velocity of 3 mm droplets was evaluated to 7.9 m/s according to the formula given in literature (Chan et al., 2009). If so the droplet penetrates into the gelling bath at a speed only 25–33% of the terminal velocity and 6–9% of the maximum corresponding kinetic energy. Increasing the height may favor the capacity of the droplet to penetrate the $CaCl_2$ gelling bath but may promote in same time a deformation due to kinetic energy of the droplet during impact with the gelling solution.

3.6. Droplet penetration into gelling bath

While the droplet hits the liquid surface, different scenarios may be observed:

- The viscosity of the droplet is too low and the droplet spread out on the liquid surface. This was not observed with alginate droplets falling in a $CaCl_2$ gelling bath even with high glycerol concentrations. This was observed for example while dropping low viscosity oil in alginate solution.
- The droplet deforms the liquid surface but its energy is not strong enough to break the surface resistance and the droplet remains tied to the surface (Fig. 5b).
- The kinetic energy of the droplet is sufficient to break the liquid surface. The droplets cross in the liquid surface with more or less deformation.

The effects of the viscosities of both alginate and $CaCl_2$ solutions on penetration process were examined. The penetration depths of droplets are given in Table 2 and Fig. 8a. Penetration depth of droplets decreased as the viscosity of $CaCl_2$ solution increased. The $CaCl_2$ solution viscosity brakes down droplet velocity, not allowing them to penetrate deeply.

The penetration depth increases as the alginate solution viscosity increases. It may be expected that for higher viscosity, the droplets are less sensitive to deformation and behave more as solid spheres. The viscosities of both alginate and $CaCl_2$ solutions have then a significant influence on penetration depth of alginate droplets into gelling bath (p < 0.05). However according to the results, it is observed that even the viscosity of alginate solution is extremely higher than viscosity of $CaCl_2$ solution (at minimum viscosity of gelling solution 20 mPa s), droplet penetration is reduced (less than 15 mm). However for viscosity of gelling solution higher than a limit (20 mPa.s), even the high viscosity of
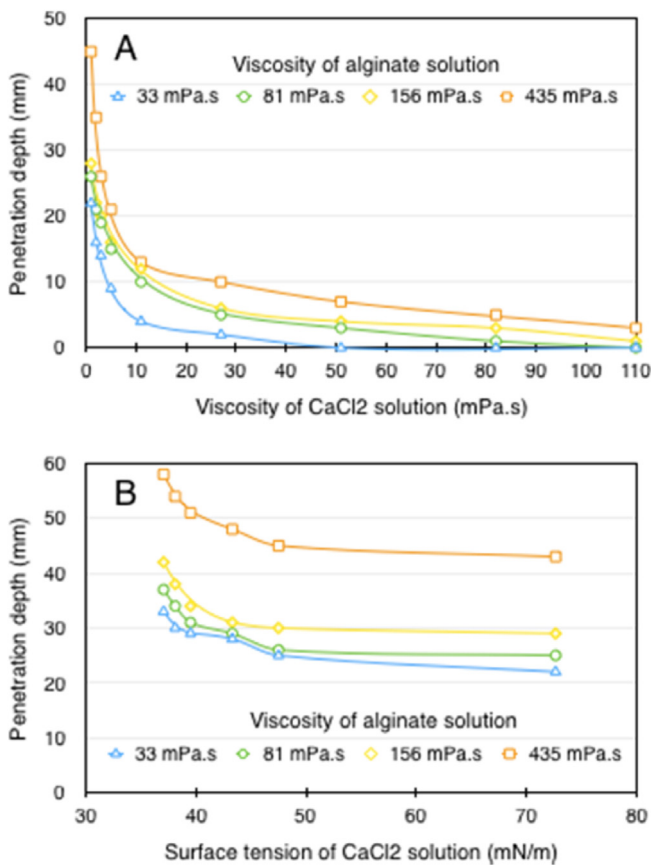
Table 2
Effect of viscosity of alginate and CaCl₂ solution on penetration depth of alginate droplets into gelling bath. All data are given as penetration depth ± SD (mm) in the table.

Viscosity of CaCl₂ solution (mPa s)	Viscosity (mPa s) of alginate solution				Mean
	33 mPa s (10 g/L)	81 mPa s (15 g/L)	156 mPa s (20 g/L	435 mPa s (30 g/L)	
1	22 ± 0.62*	26 ± 0.38	28 ± 0.35	45 ± 0.59	30.5[a]
2	16 ± 0.15	21 ± 0.53	22 ± 0.06	35 ± 0.23	23.7[b]
3	14 ± 0.28	19 ± 0.10	20 ± 0.49	26 ± 0.17	19.8[c]
5	9 ± 0.06	15 ± 0.33	16 ± 0.20	21 ± 0.43	15.3[d]
11	4 ± 0.03	10 ± 0.36	12 ± 0.10	13 ± 0.09	9.9[e]
27	2 ± 0.03	5 ± 0.18	6 ± 0.05	10 ± 0.08	5.8[f]
51	0	3 ± 0.10	4 ± 0.14	7 ± 0.12	3.4[g]
82	0	1 ± 0.03	3 ± 0.32	5 ± 0.05	2.3[h]
110	0	0	1 ± 0.08	3 ± 0.20	1[i]
Mean	7.6[A]	11.2[B]	12.6[C]	18.3[D]	

Grey area indicates the depth where spherical beads are produced.
Surface tension of the CaCl₂ gelling bath: 72,27 mN/m.
* Different lowercase letters in mean column (group comparisons were performed only regarding the viscosity of CaCl₂) and uppercase letters in mean row (group comparisons were performed only regarding the viscosity of alginate) indicate statistically significant differences at 5% ($p < 0.05$) according to Duncan's test.

Fig. 8. Alginate droplet penetration depth in CaCl₂ gelling bath versus bath viscosity (a) and surface tension (b).

alginate solution, droplet penetration is reduced (less than 15 mm) and the kinetics energy of the droplet is too small to break the gelling bath surface. This result may lead to conclude that viscosity of CaCl₂ solution is primary factor to control and optimize the penetration process.
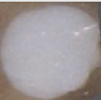
Impact of droplet alginate viscosity and Tween 20 concentrations in CaCl₂ solution is presented in Table 3 and Fig. 8b. When the surface tension of the CaCl₂ solution is constant, penetration depth of alginate droplets increased as the concentration or viscosity of alginate. Penetration depth of alginate droplets increased as the surface tension of CaCl₂ solution decreased; i.e. Tween concentration increases.

Surface tension of CaCl₂ solution has then a significant influence on penetration depth of alginate droplets into gelling bath ($p < 0.05$). It is reported that addition of a surfactant (0,1 wt-% Tween 20) supports the penetration of alginate droplets into the liquid (Haeberle, Naegele, Burger, Zengerle, & Ducrée, 2007). However, it could not totally compensate for effect of increasing of the CaCl₂ gelling bath viscosity.

3.7. Shape analysis

Fig. 9 presents the shape of the beads in function of viscosity of the alginate and CaCl₂ solution. Deformation increases as the viscosity of the gelling bath increases but could be compensated by increasing the viscosity of the alginate solution. By comparing Fig. 9 and Table 3, it was concluded that a relationship exists between the penetration depth and the sphericity of the beads. A penetration of around or higher than 15 mm is necessary to succeed in breaking up the gelling bath surface and obtain spherical beads. For lower penetration depths, either the deformation of the alginate droplet is too important or the droplet does not cross the liquid surface and remains sticking to it.

Higher droplet viscosity allows deeper penetration and more

Table 3
Effect of surface tension of CaCl₂ solution on penetration depth of alginate droplets into gelling bath. All data are given as penetration depth ± SD (mm) in the table.

Tween 20 concentration (g/L)	Surface tension of CaCl₂ solution (mN/m)	Alginate concentration (g/L)				Mean
		10	15	20	30	
0	72.27	22 ± 0.34	25 ± 0.20	29 ± 0.16	43 ± 0.29	29.9[a]
0.01	47.55	25 ± 0.36	26 ± 0.11	30 ± 0.38	45 ± 0.14	31.8[b]
0.025	43.32	28 ± 0.27	29 ± 0.76	31 ± 0.18	48 ± 0.44	34.2[c]
0.05	39.48	29 ± 0.25	31 ± 0.02	34 ± 0.60	51 ± 0.14	36.4[d]
0.1	38.08	30 ± 0.32	34 ± 0.96	38 ± 0.12	54 ± 0.39	39[e]
0.5	37.05	33 ± 0.74	37 ± 0.41	42 ± 0.26	58 ± 0.18	42.5[f]
	Mean	27.8[A]	30.5[B]	34.1[C]	50[D]	

Viscosity of the CaCl₂ gelling bath: 1 mPa s.
* Different lowercase letters in mean column (group comparisons were performed only regarding the surface tension of CaCl₂) and uppercase letters in mean row (group comparisons were performed only regarding the concentration of alginate) indicate statistically significant differences at 5% ($P < 0.05$) according to Duncan's test.

Viscosity of CaCl₂ solution (mPas)	Alginate concentration (g/L)			
	10 g/L	15 g/L	20 g/L	30 g/L
1	PD = 22 mm Φ = 0,98	PD = 26 mm Φ = 0,99	PD = 28 mm Φ = 0,99	PD = 45 mm Φ = 0,99
2	PD = 16 mm Φ = 0,94	PD = 21 mm Φ = 0,98	PD = 22 mm Φ = 0,98	PD = 35 mm Φ = 0,98
3	PD = 14 mm Φ = 0,94	PD = 19 mm Φ = 0,97	PD =20 mm Φ = 0,98	PD = 26 mm Φ = 0,98
5	PD = 9 mm Φ = 0,92	PD = 15 mm Φ = 0,97	PD = 16 mm Φ = 0,97	PD = 20 mm Φ = 0,98
11	PD = 4 mm Φ = 0,80	PD = 10 mm Φ = 0,95	PD = 12 mm Φ = 0,94	PD = 13 mm Φ = 0,96
27	PD = 2 mm Φ =0,62	PD = 5 mm Φ = 0,88	PD = 6 mm Φ = 0,88	PD = 10 mm Φ = 0,91
82		PD = 1 mm Φ = 0,77	PD = 3 mm Φ = 0,80	PD = 5 mm Φ = 0,90
110			PD = 1 mm Φ = 0,79	PD = 3 mm Φ= 0,86

$CaCl_2$

Fig. 9. Influence of the viscosity of alginate solution and $CaCl_2$ gelling bath solution on the alginate bead shape. Dark grey zone indicates spherical or slightly oval beads (Φ > 0,95), light grey zone indicates oval to pear shape (Φ > 0,90).

spherical beads are obtained even for higher gelling bath viscosity (Fig. 9). These results showed good relevance with the previous findings (Chan, 2011; Chan et al., 2009; Chen & Chen, 2007; Dohnal & Štěpánek, 2010).

Addition of a certain amount of surfactant enhances alginate droplet penetration by decreasing the surface tension. If surface tension of gelling solution (CaCl$_2$) decreases, even for a smaller depth penetration, the droplet is able to cross the liquid surface. The shape deformation at liquid surface due to impact decreases. In this study, all beads produced when surfactant was added to the CaCl$_2$ solution were spherical. Therefore, the surface tension of receiving solution may be adjusted by adding surfactants, and may prevent shape deformations.

4. Conclusion

Ca-alginate beads were produced via ionotropic gelation principle using dripping technique. During the study, concentration and viscosity of alginate solution was modified. Also, by modifying viscosity and surface tension of CaCl$_2$ solution, different solutions were prepared and various Ca-alginate bead batches were produced. Effect of these physical properties (viscosity, surface tension) of solutions on penetration depth of alginate droplets, and on size and shape of Ca-alginate beads were investigated. All steps of dripping (droplet formation, fall of droplets and penetration) were observed by using a high-speed camera.

Viscosity of alginate solutions has a statistically significant but limited impact on droplet diameter. Alginate flow rate and nozzle size have a stronger impact on the droplet diameter.

As droplet detaches from the nozzle, it gets a spherical shape in less than 500 ms and less than 2.5 cm under the nozzle. One may then assume that in most cases, penetration in the gelling bath is the main cause of the bead deformation.

Penetration depth decreases when alginate viscosity decreases and when CaCl2 gelling bath viscosity increases. If the penetration depth is too small, the CaCl2 gelling bath surface is not broken/open and droplets remain attach to its surface.

Spherical beads are obtained first if the droplets are able to cross the CaCl$_2$ gelling bath surface but also the impact with the liquid surface does not deform the droplet. The second condition is improved especially if the viscosity of the alginate solution is higher.

This paper shows that using high-speed camera may really help defining optimum conditions to realize good dripping techniques. In future, research may continue to analyze the process more deeply and extend the study to more complex process like electro-dripping, co-extrusion, etc. Also more experiments should be conducted on penetration step of dripping to promote penetration of droplets into receiving solution.

References

Akhtar, M., Murray, B. S., Afeisume, E. I., & Khew, S. H. (2014). Encapsulation of flavonoid in multiple emulsion using spinning disc reactor technology. *Food Hydrocolloids, 34*, 62—67.

Belščak-Cvitanović, A., Bušić, A., Barišić, L., Vrsaljko, D., Karlović, S., Špoljarić, I., et al. (2016). Emulsion templated microencapsulation of dandelion (Taraxacum officinale L.) polyphenols and β-carotene by ionotropic gelation of alginate and pectin. *Food Hydrocolloids, 57*, 139—152.

Boström, M., Kunz, W., & Ninham, B. W. (2005). Hofmeister effects in surface tension of aqueous electrolyte solution. *Langmuir, 21*(6), 2619—2623.

Chan, E.-S. (2011). Preparation of Ca-alginate beads containing high oil content: Influence of process variables on encapsulation efficiency and bead properties. *Carbohydrate Polymers, 84*(4), 1267—1275.

Chan, E.-S., Lee, B.-B., Ravindra, P., & Poncelet, D. (2009). Prediction models for shape and size of ca-alginate macrobeads produced through extrusion—dripping method. *Journal of Colloid and Interface Science, 338*(1), 63—72.

Chan, E.-S., Lim, T.-K., Ravindra, P., Mansa, R. F., & Islam, A. (2012). The effect of low air-to-liquid mass flow rate ratios on the size, size distribution and shape of calcium alginate particles produced using the atomization method. *Journal of Food Engineering, 108*(2), 297—303.

Chen, M. J., & Chen, K. N. (2007). Applications of probiotic encapsulation in dairy products. *Encapsulation and Controlled Release Technologies in Food Systems*, 83—112.

Doherty, S., Gee, V., Ross, R., Stanton, C., Fitzgerald, G., & Brodkorb, A. (2011). Development and characterisation of whey protein micro-beads as potential matrices for probiotic protection. *Food Hydrocolloids, 25*(6), 1604—1617.

Dohnal, J., & Štěpánek, F. (2010). Inkjet fabrication and characterization of calcium alginate microcapsules. *Powder Technology, 200*(3), 254—259.

Gibbs, F., Kermasha, S., Alli, I., Mulligan, C. N., & Bernard. (1999). Encapsulation in the food industry: A review. *International Journal of Food Sciences and Nutrition, 50*(3), 213—224.

Haeberle, S., Naegele, L., Burger, R., Zengerle, R., & Ducrée, J. (2007). Alginate micro-bead fabrication on a centrifugal microfluidics platform. In *Micro electro mechanical systems, 2007. MEMS. IEEE 20th international conference on* (pp. 497—500). IEEE.

Harkins, W. D., & Brown, F. (1919). The determination of surface tension (free surface energy), and the weight of falling drops: The surface tension of water and benzene by the capillary height method. *Journal of the American Chemical Society, 41*(4), 499—524.

Kierstan, M., & Bucke, C. (2000). The immobilization of microbial cells, subcellular organelles, and enzymes in calcium alginate gels. *Biotechnology and Bioengineering, 67*(6), 726—736.

Knezevic, Z., Bobic, S., Milutinovic, A., Obradovic, B., Mojovic, L., & Bugarski, B. (2002). Alginate-immobilized lipase by electrostatic extrusion for the purpose of palm oil hydrolysis in lecithin/isooctane system. *Process Biochemistry, 38*(3), 313—318.

Koupantsis, T., Pavlidou, E., & Paraskevopoulou, A. (2014). Flavour encapsulation in milk proteins—CMC coacervate-type complexes. *Food Hydrocolloids, 37*, 134—142.

Lee, B.-B., Ravindra, P., & Chan, E.-S. (2008). A critical review: Surface and interfacial tension measurement by the drop weight method. *Chemical Engineering Communications, 195*(8), 889—924.

Lević, S., Lijaković, I. P., Đorđević, V., Rac, V., Rakić, V., Knudsen, T.Š., et al. (2015). Characterization of sodium alginate/D-limonene emulsions and respective calcium alginate/D-limonene beads produced by electrostatic extrusion. *Food Hydrocolloids, 45*, 111—123.

Li, C., Wang, J., Shi, J., Huang, X., Peng, Q., & Xue, F. (2015). Encapsulation of tomato oleoresin using soy protein isolate-gum aracia conjugates as emulsifier and coating materials. *Food Hydrocolloids, 45*, 301—308.

Moghadam, H., Samimi, M., Samimi, A., & Khorram, M. (2008). Electro-spray of high viscous liquids for producing mono-sized spherical alginate beads. *Particuology, 6*(4), 271—275.

Nakauma, M., Funami, T., Fang, Y., Nishinari, K., Draget, K. I., & Phillips, G. O. (2016). Calcium binding and calcium-induced gelation of sodium alginate modified by low molecular-weight polyuronate. *Food Hydrocolloids, 55*, 65—76.

Nussinovitch, A. (2010). Physical properties of beads and their estimation. In A. Nussinovitch (Ed.), *Polymer macro-and micro-gel Beads: Fundamentals and applications* (pp. 1—25). Springer.

Pennell, K., Karagunduz, A., Yeh, D., Martin, C., Chang, E., & Pavlostathis, S. (2000). Influence of nonionic surfactants on the bioavailability of chlorinated benzenes for microbial reductive dechlorination. In *Abstracts of papers of the american chemical society, 220*1155 16TH ST, NW, WASHINGTON, DC 20036 USA: American Chemical Society (pp. U342—U342).

Rajabi, H., Ghorbani, M., Jafari, S. M., Mahoonak, A. S., & Rajabzadeh, G. (2015). Retention of saffron bioactive components by spray drying encapsulation using maltodextrin, gum Arabic and gelatin as wall materials. *Food Hydrocolloids, 51*, 327—337.

Schrooyen, P. M., van der Meer, R., & De Kruif, C. (2001). Microencapsulation: Its application in nutrition. *Proceedings of the Nutrition Society, 60*(04), 475—479.

Ubbink, J., & Krüger, J. (2006). Physical approaches for the delivery of active ingredients in foods. *Trends in Food Science & Technology, 17*(5), 244—254.

Yang, Y., & McClements, D. J. (2013). Encapsulation of vitamin E in edible emulsions fabricated using a natural surfactant. *Food Hydrocolloids, 30*(2), 712—720.

Zeeb, B., Saberi, A. H., Weiss, J., & McClements, D. J. (2015). Formation and characterization of filled hydrogel beads based on calcium alginate: Factors influencing nanoemulsion retention and release. *Food Hydrocolloids, 50*, 27—36.